# Single-Tube and Multi-Turn Coil Near-Field Wireless Power Transfer for Low-Power Home Appliances

**Aqeel Mahmood Jawad** [1,2,*]**, Rosdiadee Nordin** [1] **, Sadik Kamel Gharghan** [3]**, Haider Mahmood Jawad** [1,2]**, Mahamod Ismail** [1] **and Mahmood Jawad Abu-AlShaeer** [4]

1   Centre of Advanced Electronic & Communication Engineering, Faculty of Engineering and Built Environment, Universiti Kebangsaan Malaysia, UKM Bangi, Selangor 43600, Malaysia; adee@ukm.edu.my (R.N.); haider_mahmood2003@yahoo.com (H.M.J.); mahamod@ukm.edu.my (M.I.)
2   Department of Computer Communication Engineering, Al-Rafidain University College, Filastin, Baghdad 10064, Iraq
3   Department of Medical Instrumentation Techniques Engineering, Electrical Engineering Technical College, Middle Technical University (MTU), Al Doura, Baghdad 10022, Iraq; sadiq_gharghan@yahoo.com
4   Department of Statistic, Al-Rafidain University College, Filastin, Baghdad 10064, Iraq; mahmoud_juad@yahoo.com
*   Correspondence: aqeel_mahmood_1986@yahoo.com; Tel.: +60-105-188-509

**Abstract:** Single-tube loop coil (STLC) and multi-turn copper wire coil (MTCWC) wireless power transfer (WPT) methods are proposed in this study to overcome the challenges of battery life during low-power home appliance operations. Transfer power, efficiency, and distance are investigated for charging mobile devices on the basis of the two proposed systems. The transfer distances of 1–15 cm are considered because the practicality of this range has been proven to be reliable in the current work on mobile device battery charging. For STLC, the Li-ion battery is charged with total system efficiencies of 86.45%, 77.08%, and 52.08%, without a load, at distances of 2, 6, and 15 cm, respectively. When the system is loaded with 100 Ω at the corresponding distances, the transfer efficiencies are reduced to 80.66%, 66.66%, and 47.04%. For MTCWC, the battery is charged with total system efficiencies of 88.54%, 75%, and 52.08%, without a load, at the same distances of 2, 6, and 15 cm. When the system is loaded with 100 Ω at the corresponding distances, the transfer efficiencies are drastically reduced to 39.52%, 33.6%, and 15.13%. The contrasting results, between the STLC and MTCWC methods, are produced because of the misalignment between their transmitters and receiver coils. In addition, the diameter of the MTCWC is smaller than that of the STLC. The output power of the proposed system can charge the latest smartphone in the market, with generated output powers of 5 W (STLC) and 2 W (MTCWC). The above WPT methods are compared with other WPT methods in the literature.

**Keywords:** electromagnetic field; mobile device; inductive coupling; near-field; single-tube loop coils; multi-turn copper wire coil; wireless power transfer

## 1. Introduction

Wireless charging has recently found its way into the commercial market for electric vehicle charging facilities, mobile phones, portable laptops, smart watches, and drones [1]. Mobile phones and laptop computers are two of the devices that use wireless power transfer (WPT) technology the most. In the last 20 years, most mobile phones, portable laptops, electric vehicles, drones, and electronic devices have still been operating with batteries, despite their heavy weight, the nuisance of charging cables, and the long charging times. However, high-data-rate wireless communication

and high-performance low-power system designs continue to drive the expansion of the market for mobile electronic devices. The demand for WPT systems has increased because of these issues and other battery shortcomings. WPT technologies have recently been developed for mobile electronic devices and electric vehicles to overcome the limitations of battery power transfer [2].

Wireless charging eliminates the need for cables that are typically required to charge mobile phones and cordless appliances. A wireless charger allows the battery in any battery-powered appliance to be charged when the device is placed close to a wireless power transmitter or a designated charging station. Consequently, the appliance casing can be sealed completely or even waterproofed. In addition to providing inherent convenience, wireless charging can enhance reliability. The charging plug of an appliance can easily be damaged by incidents, such as the inadvertent use of the wrong adapter. The principle behind wireless charging is the well-known Faraday's law of induced voltage, which is commonly used in motors and transformers [3]. The charging process requires that the user place a charging pad in direct contact with the device to be charged, thus enabling wireless charging. However, the previous work on WPT has not achieved this goal. Transmitting a significant amount of power wirelessly is normally accomplished by magnetic fields, which are extremely directional and have rapidly dropping values with increasing distance. Consequently, high-technology phone chargers are limited to distances of a few centimeters and require the phone to be perfectly aligned with the charging pad. Substantial distance coverage and elastic wireless charging are beneficial to users. Phone chargers that work at distances of approximately 15 or 20 cm [4] and can charge phones and laptops anywhere are needed. A charging pad can be placed between two small tables to charge a phone [5]. Transfer distance and system efficiency are important concerns in inductive power transfer (IPT) systems. Several IPT tests have shown high power transfer efficiencies that exceed 80% at distances of 1–10 cm [6,7]. However, one of the main limitations of IPT systems, such as the traditional single receiver, is the difficulty in handling heavy load requirements. Therefore, the multiple-receiver approach may be a promising solution to the long-distance demands of wireless charging applications [8].

In this work, the transfer distance, power, and efficiency of a wireless charging system, based on a single-tube loop coil (STLC) and a multi-turn copper wire coil (MTCWC) inductive coupling-based WPT, are developed and proposed. In addition, the proposed method is compared with several types of wireless charging systems according to the previous work of other researchers. The contributions of the present study are as follows:

(i.)　Two new systems (STLC and MTCWC) are designed and implemented, based on a parallel to parallel compensation capacitors topology.

(ii.)　The performance metrics of the two systems are explored in terms of transfer distance, output power, transfer efficiency, output voltage, and operating frequency.

(iii.)　A comparison between the two proposed systems is conducted in terms of performance metrics, with and without different resistive loads.

(iv.)　The battery-charging function of a mobile device is confirmed using the two systems.

(v.)　The proposed systems outperform the other methods in the literature, in terms of transfer distance, output power, and efficiency, according to the comparative results.

The remainder of this paper is structured as follows. Section 2 presents the review of related literature. Section 3 presents low-power inductive power transfer applications. Section 4 describes and analyzes the system design of STLC and MTWCW. Section 5 introduces the experimental topologies of both systems. Section 6 presents the performance measurements and the results of the STLC and MTCWC systems, in terms of power and efficiency with respect to distance. Section 7 discusses the comparison of the two systems with those presented in the previous literature, in terms of frequency, output power, transfer efficiency, transfer distance, and transmitter and receiver coil design. Finally, Section 8 concludes this research.

## 2. Related Works

In a review by Pinuela et al. [9], a copper piping WPT system, comprising three primary transmitters and five secondary receiver coils, was designed. The authors adopted field-shaping techniques that are based on an efficient IPT system, capable of transmitting energy with a DC-to-load efficiency of above 77% at 6 MHz across 30 cm. This percentage is the highest DC-to-load efficiency achieved for an IPT system without introducing restrictive coupling factor enhancement techniques. Therefore, class E amplifiers have been identified as ideal drivers for IPT applications. However, the power handling capability of these amplifiers, at tens of megahertz, is a crucial limiting factor because load and inductor characteristics are set by the requirements of resonant inductive systems. Park et al. [10] proposed a compact resonant reactive shielding coil topology for reducing EMF in near-field WPT mobile device applications. The shielding coil utilizes closed-loop and matching capacitors and dramatically reduces the leakage magnetic field in a WPT system. The shield coils were classified into four types according to measured and simulated transfer efficiencies:

(i.)　Without shield, which had simulated and measured transfer efficiencies of 98.3% and 96.2%, respectively;

(ii.)　Active shield, which had simulated and measured transfer efficiencies of 79.3% and 75.1%, respectively;

(iii.)　Non-resonator shield, which had simulated and measured transfer efficiencies of 97.1% and 95%, respectively; and

(iv.)　Prop-resonator reactive shield, which had simulated and measured transfer efficiencies of 93.6% and 90.2%, respectively, under a 6.78-MHz frequency and 10-W input power.

The results of their analytical solutions and simulations are consistent with those obtained by measurement.

Feng et al. [11] proposed a wireless charging bowl method with an omnidirectional power transfer concept. The omnidirectional WPT system is based on a finite element analysis simulation and a numerical model. In addition, the authors suggested a new transmitter coil structure, with a preferred omnidirectional magnetic field, constructed three coils, with an operating frequency of 6.78 MHz, and inductor-capacitor-inductor (LCL) resonant converters to drive the transmitter coils and generate an omnidirectional magnetic field, and compared two modulation methods, namely, concentrated and distributed windings. Their results showed that the two systems could not yield the desired omnidirectional magnetic field. Goguri et al. [12] presented a simple theoretical model, supported by experimental evidence, to maximize the transfer efficiency of WPT with a single receiver and multiple transmitters. The authors described the simple design of the utilized multiple transmitter coils and the receiver coil. They also investigated a multiple-input–single-output transmit power source with a near-field inductive coupling WPT system. Several transmitters were utilized to potentially enable the system to direct the transmitted power to the receiver from a phased array through a process similar to beamforming. This model aims to construct a simple experimental setup with 27% efficiency. The advantage of the modeling in the current work is its economical representation, in which the number of unknown parameters can be considerably smaller than that of the lumped circuit elements required for a complete and accurate representation, as reported in a previous work that used lumped resistor-inductor-capacitor (RLMC) circuits.

Yang et al. [13] designed a high-*Q*-factor flexible coil, called the planar-Litz coil, to replace the single-strand coils in wireless energy transfer systems. Two types of layer Litz wire structure coils were used to construct a four-coil magnetic resonance coupling system. The transfer distance and efficiency of the proposed four-coil WPT were compared with those of a two-coil WPT. Their results showed that the coupling efficiency could improve by 40%. When two resonant coils were added to the transfer system, the transfer efficiency increased to 78% at a transfer distance of 0.5 cm. The performance of the resonant coil system was 20% better than the traditional system (i.e., without a resonant coil). Their results also showed that the *Q*-factor of the Litz structure coils had a higher *Q*-factor

than that of the single-strand coils. Therefore, increasing the number of coils increases the transfer distance and cost, while decreasing the transfer efficiency. Jadidian and Katabi [5] highlighted the benefits of multiple-input–multiple-output (MIMO) WPTs, which can be used to charge mobile phones remotely, even in clothing pockets. Therefore, a novel system was presented to charge portable devices, such as cell phones and laptops, at distances of 0.5–40 cm, with a power transfer efficiency of 89%, regardless of device position and orientation. This work successfully demonstrated the construction of the MIMO and its capacity to charge an iPhone and other smartphones at a single frequency of 1 MHz while in the pockets of users. Jonah et al. [14] optimized a three-loop misalignment structure for WPT through strongly coupled magnetic resonance (SCMR) with a misalignment insensitivity performance and focused on the design of wireless power systems that are based on the SCMR method. Furthermore, the power transfer efficiency was improved in several directions. The authors compared the misalignment-insensitive SCMRs in the three- and two-loop structures. Their results showed that the measured and simulated transfer efficiencies of the three-loop structure were 60% and 70%, respectively. Similarities and differences were identified between the standard SCMR and the two misalignment-insensitive SCMR models (i.e., two-/three-loop structures). The SCMR power transfer efficiency was above 60% in the misalignment range of 0–90°. However, the angular and lateral misalignments were better than those of the typical SCMR elements, utilized for WPT applications.

Ye et al. [15] proposed a new method of inductive coupling that can convey energy at a relatively greater distance than the conventional method. The researchers designed a new U-coil system technique that comprises three coils, namely, primary, secondary, and relay coils. The relay coil is between the secondary and primary coils, where energy can pass. This method (i.e., U-coil WPT) was established to achieve a better energy transfer efficiency than that of the two-coil method. The U-coil approach achieved a power transfer of 100 cm between the source and destination coils, with an operating frequency of 85 kHz. The U-coil method attained an energy transfer efficiency that was 66% better than that of the two-coil method. Kim et al. [16] presented a WPT system that utilizes a bowl-shaped transmitting coil (B-STxC) to charge small electronics, such as hearing aids and wearable electronic devices. They suggested three-coil WPT systems. An exact mutual inductance calculation method was ensured between the circular and rectangular loops. The B-STxC comprises spiral and conical–helical coils. The electronic device, which is to receive power, is to be placed in the B-STxC and charged with spatial freedom. The use of a compact box-like receiving coil with ferrite sheets in the box improved the magnetic coupling. The proposed system could charge a Li–ion battery uniformly in the parallel arrangement, with an overall efficiency of 30%. In the proposed design, the Rx impedance matching for enhancing the power transfer efficiency was addressed without needing additional impedance matching circuits. Fu et al. [17] compared the cross-coupling between two adjacent receiver coils and explored the characteristics that affected the power transfer. Two thickness values of the wire coil were adopted between the transmitter and multiple-receiver coils. The two delivered powers (i.e., P1 and P2) of the two receivers achieved transfer efficiencies of 52.8% and 53.1% at an operating frequency of 13.56 MHz.

Rooij and Mirenda [18] proposed a new topology that was supported by experimental verification and demonstrated excellent performance at both low (Qi and PMA standards) and high (A4WP standard) frequencies. They also presented a simple Enhancement-Mode Gallium Nitride field effect transistor (e-GaN FET)-based single amplifier topology, capable of operating in accordance with all mobile device wireless power standards at a frequency range of 100 kHz. The output powers of the three standards, namely, A4WP, Qi, and PMA, were compared to obtain the high and low frequencies with a low power transfer range of 1–70 W for A4WP, 5 and 10 W for Qi, and 5 W for PMA at a standard frequency of 6.78 MHz. Mittleider et al. [4] presented a novel unmanned aerial vehicle (UAV)-based technique for charging wireless sensor networks (WSNs). The UAV could be precisely positioned at 15 cm and relied on magnetic resonant sensors, in which the global positioning system is imprecise and requires a line-of-sight between the satellite and receiver. However, the transfer efficiency could be improved by placing the conveying coil (fixed on the UAV) and reception coil

(fixed on the sensor node) adjacent to one another. Accordingly, a charging power of 5.49 W, with 6 cm between the transmitting and receiving coils, is sufficient to charge the battery of the WSN at a remote site. Rozman et al. [19] presented a novel method, featuring a resonant two-loop WPT system. A compensation inductor, combined with two-loop coils (i.e., receiver and transmitter), was proposed to reduce the sizes of the two coils significantly. Consequently, the size and weight of the transmitter and receiver could be minimized. The performance of the proposed design was confirmed by the similarities between the simulation and experimental results. The prototype achieved a high transfer efficiency of 93%. The proposed design could minimize the transmitter and receiver loop lengths to 3 and 4 mm, and these lengths were remarkably shorter than those in the traditional design, which were 15 and 20 mm, respectively. In addition, the weight of the transmitter was reduced to 1.58 g, whereas the weight under the conventional design was 7.37 g. Meanwhile, the receiver weight was improved, decreasing from 8.63 g to 1.78 g. The overall reduction in prototype size was 80%. However, the reduction in size, weight, and cost reduced system efficiency. Furthermore, the transfer distance, which is influenced by the coupling factor between the transmitter and receiver, and the maximum power could be transferred between the two coils when the coupling factor was 0.003.

Device-to-device WPT has been proposed in recent studies [20]. Power transfer is accomplished based on inductive coupling with two symmetrical PCB coils (4 cm outer diameter) to charge wearable/portable devices. Based on the fabrication of the complementary metal oxide semiconductor (CMOS) technology, a cross-connected WPT was introduced by Mao et al. [21]. CMOS fabrication is achieved at 0.35 μm, with a total area of 3.92 mm$^2$. Consequently, the total efficiency of 78.1% can be achieved, with a maximum output power of 2.7 W, at an air gap of 23 mm and frequency of 6.78 MHz.

The present study aims to investigate the transfer power, efficiency, and distance of an IC WPT that is based on the proposed STLC and MTCWC methods. Both systems are compared with models in related articles, in terms of various performance metrics.

## 3. Inductive Power Transfer for Low Power Home Appliances

The applications of IPT techniques have been highlighted in several studies. Some of these applications, which are relevant to low-power home appliances, can be summarized as follows.

(i.) Users of smartphones, portable media players, digital cameras, tablets, and wearable devices request easy-to-use solutions, increased freedom of positioning, and reduced charging times. These applications typically require 2–15 W and prefer multi-standard interoperability. Wireless charging can coexist with near-field communication (NFC) and Bluetooth, thereby allowing for innovative solutions. For example, paired phones can charge one another when placed back-to-back, after the appropriate host and client have negotiated.

(ii.) Accessories, such as headsets, wireless speakers, mice, and keyboards, can benefit from WPT. Plugging charging cables into the tiny connectors of small devices is an impediment to robust design. For example, Bluetooth headsets must be sweat-proof to survive in gyms, and only wireless charging can make this characteristic possible.

(iii.) Public-access charging terminals, where charging pads (transmitters) are deployed in the public domain, require safe and secure systems. However, smart charging systems can offer considerably more than stand-alone charging solutions, thereby enabling quick network connectivity and creating billable charging stations when desired. Many coffee shops, airport kiosks, and hotels support these scenarios. Furniture manufacturers also incorporate discreet wireless power transmitters into their end and side tables.

(iv.) Computer systems, such as laptops, notebooks, ultra-books, and tablet PCs, are all candidates for wireless charging, as either hosts or clients. The possibilities are endless.

(v.) In cabin automotive applications, a wireless charger is ideal for charging mobile phones and key fobs. Such chargers can be placed either on the dash or in the center console of the car, without inconvenient wires protruding from cigarette lighter sockets. Moreover, combining NFC with

wireless charging not only enables users to charge their phones but also automatically connects these devices to the Wi-Fi and Bluetooth networks of their cars, without undergoing any specific setup process. Bluetooth and Wi-Fi require authentication to connect phones to car electronics.

(vi.) In miscellaneous applications, wireless chargers are now used for devices with batteries, such as game consoles and TV remotes, cordless power tools, cordless vacuum cleaners, soap dispensers, hearing aids, and pacemakers. Wireless chargers are also capable of charging super capacitors or any device that is traditionally powered by a low-voltage power cable [22].

(vii.) Wireless charging can be used to charge WSNs and drones, which are used for different applications [4].

## 4. Methodology

### 4.1. Proposed STLC and MTCWC System

The proposed system, which consists of one source (transmitter) and two receivers, is shown in Figure 1. The transmitter includes the STLC coil (Figure 1, Part A). The first receiver coil is an STLC, while the second receiver is an MTCWC (Figure 1, Parts B and C, respectively). The two receivers are used to charge home appliances in this study. Two separate charging circuits are considered, that is, the STLC receiver can be used to charge device batteries requiring 4 W (e.g., a Nokia 1280 mobile phone), while the MTCWC receiver can be used to charge low-power home appliances (e.g., headphones, shavers, and toothbrushes). In addition, the proposed system can simultaneously charge two devices. The energy is transferred from the source coil to the two receiver coils. The proposed design of the tube coil, for the transmitter and receiver of the STLC circuit, is shown in Figure 2. The tube coils are configured as closed single loops of coiled electrical conductors. The basic principle of the tube and multi-turn coils is the same as that of WPTs. An example of the proposed STLC design is shown in Figure 3a, while an example of the proposed MTCWC design is shown in Figure 3b. The source or transmitting circuit includes an oscillator circuit, which generates 1 MHz. This circuit generates oscillation with two MOSFET transistors (IRFP250N), two general-purpose diodes (1N4008), a parallel coupling capacitor, and two resistors. The load coils (i.e., single tube and multi-turn) can be used to pass the energy to the load through the bridge rectifiers and voltage regulators. Here, the battery can be used as a load for different applications. In this work, 1 MHz is adopted to improve performance and avoid a large coil size of the transmitter and receiver, and consequently to realize a high transfer distance and efficiency. The challenges for usage (100–200 kHz) can be summarized as follows: (i) The transfer efficiency is significantly lower at a lower frequency, compared to that at a high frequency, as reported in [23], where the reference adopted an optimized control method; and (ii) the size of the transmitter and receiver coils increases with low frequencies, as Jiang et al. [24], who adopted a low-frequency WPT technology, indicate.

In general, four types of coupling or compensation capacitor topologies exist, namely, parallel to parallel, series to series, parallel to series, and series to parallel for primary and secondary coils [25]. In this work, we considered the parallel to parallel topology for the following reasons:

(i.) In series coupling capacitors, the effect of the parasitic shunt capacitance of the coil is negligible because it has a small value, whereas the effect should be considered in a parallel connection because parallel coupling capacitors cancel the effect of the small value of the parasitic shunt capacitance [9];

(ii.) To obtain a more flexible technique (i.e., resonant frequency control technique), a discrete tuning variable parallel capacitor or parallel inductor with a receiver coil can be used [26];

(iii.) The output transfer voltage, with a parallel coupling capacitor in the secondary coil, is considerably higher than that with a series coupling capacitor [27];

(iv.) The transfer efficiency of the parallel topology is better than the series topology [28], where the transfer efficiency is 95% at 100 Ω load resistance;

(v.) The parallel topology has a higher voltage boosting property than the series topology [26];

(vi.) Many researchers have adopted parallel coupling capacitors in the design of the WPT prototype [29–32]. From the above discussion, we can conclude that the parallel topology is better than the series topology.

The adopted parameters of the source and load circuits of the STLC system are illustrated in Table 1. The method in the current work is expected to yield a better transfer distance and efficiency between the source and load coils than those in previous studies that adopted different topologies.
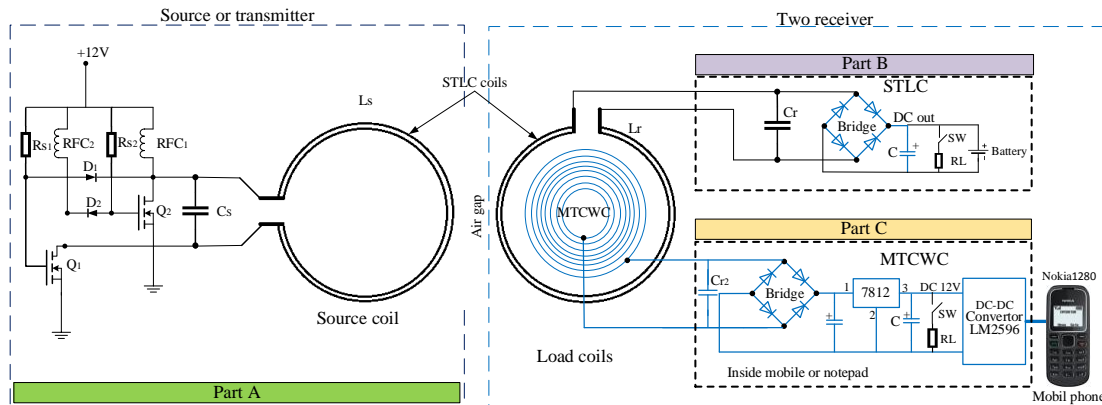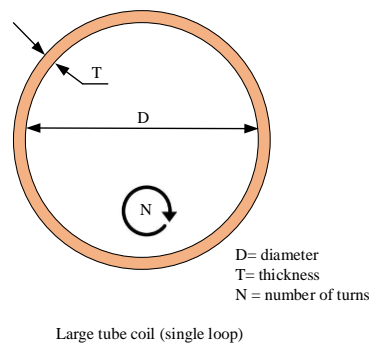


**Figure 1.** Proposed Single-tube loop coil (STLC) and multi-turn copper wire coil (MTCWC) systems.



D= diameter
T= thickness
N = number of turns

Large tube coil (single loop)

**Figure 2.** The shape of STLC.



Thickness of tube coil in mm

The dimeter of coil = 30 cm

5.7 cm

5.3 cm

(**a**)          (**b**)
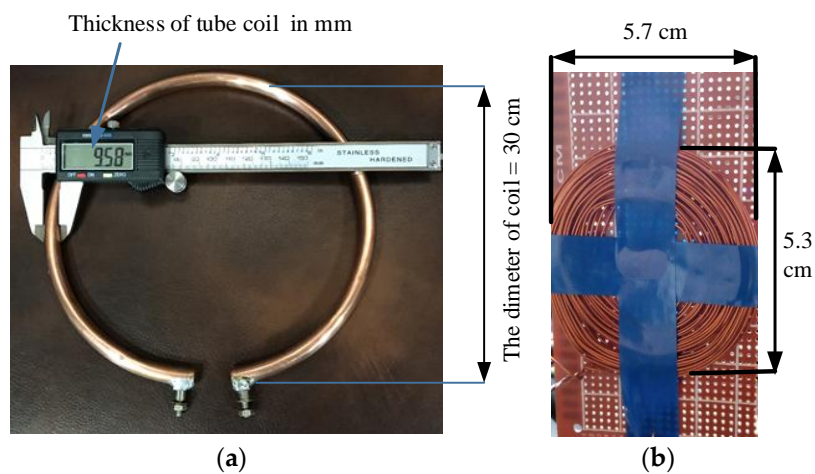
**Figure 3.** (**a**) Example of STLC and (**b**) MTCWC design.

**Table 1.** Single-tube loop coil (STLC) Parameters.

| Parameters | Value |
|---|---|
| Input voltage (E/Volt) | 12 |
| Operating frequency (f/MHz) | 1 |
| Inductance of transmitter coil (RFC1/µH) | 100 |
| Inductance of transmitter coil (RFC2/µH) | 100 |
| Compensating capacitor of transmitter coil (Cs/pf) | 300 |
| Compensating capacitor of receiver coil (Cr/pf) | 300 |
| Load resistance (RL/Ω) | 20, 50, 100 |
| Resistances (Rs1/Ω) | 50 |
| Resistances (Rs2/Ω) | 50 |

*4.2. Proposed Systems Analysis*

The source/load and its equivalent circuit model are shown in Figure 4a,b, respectively. Equation (1) illustrates the source and receiver circuits tuned at the same frequency ($f_o$) [33].

$$f_o = \frac{1}{2\pi\sqrt{L_s C_s}} = \frac{1}{2\pi\sqrt{L_r C_r}},$$

(1)

where $L_s$ and $L_r$ are the inductances of the source and the receiver, and $C_s$ and $C_r$ are the capacities of the source and the receiver, respectively.

In the current work, the adopted values of $L_s$, $L_r$, $C_s$, and $C_r$ (Table 1) yield a resonant frequency of approximately 1 MHz.
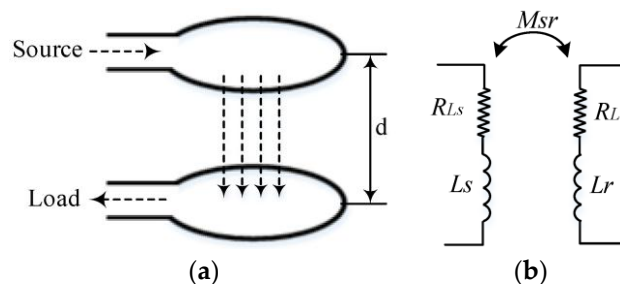


**Figure 4.** Proposed system with (**a**) source/load and (**b**) equivalent circuit model.

To increase the power transfer efficiency and capacity, a tuned $L_C$ resonator circuit is used in the source and the receiver (Figure 5). Based on the circuit shown in Figure 5, the steady-state equations for the current and voltage can be computed for each branch and node in the source and receiver circuits. Kirchhoff's voltage law can be applied to this circuit. Consequently, the transfer efficiency ($\eta$) can be calculated as follows [28]:

$$\eta = \frac{P_L}{P_S} = \frac{|I_{RL}|^2 R_L}{|I_{LS}|^2 R_{LS} + |I_{Lr}|^2 R_{Lr} + |I_{RL}|^2 R_L}$$

(2)

If the load resistance ($R_L$) is greater than ($f_o L_r$), and the resonant frequencies $f_{o1}$ and $f_{o2}$ of the two tanks are equal, as in our case, where the adopted resistive load is $R_L$ = 100 Ω and $f_{o1} = f_{o2}$ = 1 MHz, then the adopted resistive load is clearly greater than the multiplication of $f_o L_r$, which is equal to 95. Then, Equation (2) of the efficiency of the STLC and MTCWC circuits at the tuned frequency is simplified as follows [28]:

$$\eta \approx \frac{1}{1 + \frac{R_L R_{LS}}{(2\pi f_o)^2 M_{sr}^2 \left[1 + (2\pi f_o)^2 C_r^2 R_L^2\right]} + \frac{R_L R_{Lr}}{(2\pi f_o)^2 L_r^2}}$$

(3)

According to Equation (3), the transfer efficiency $\eta$ is a function of the mutual inductance between the source and receiver coils ($M_{sr}$), the resonant frequency ($f_o$), the self-inductance of the receiver coil ($L_r$), the resistors of the source and receiver coils (i.e., $R_{LS}$ and $R_{Lr}$), and the load resistor ($R_L$). The self-inductance of the receiver coil, resonant frequency, and mutual inductance between the two coils should be increased to achieve a high transfer efficiency, while the resistor value of the coils (i.e., $R_{LS}$ and $R_{Lr}$) should be decreased.
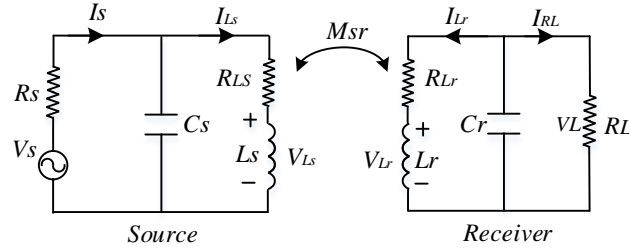


**Figure 5.** Equivalent circuit model of wireless power transfer (WPT).

### 4.3. Conjugate Image Impedance

In our work, a parallel-parallel topology is considered for the resonators on the source and receiver coils. In addition, the capacitor $C_S$ is connected in parallel with the inductor $Ls$, and the capacitor $Cr$ is connected in parallel with the inductor $Lr$ (Figure 5).

Subsequently, the impedance matrix ($Z_{pp}$) can be expressed for the two port networks (i.e., port 1 and port 2), based on [34], as follows:

$$Z_{PP} = \begin{pmatrix} \frac{Q_1}{Q_1 Q_2 k^2 + 1} - j & -\frac{j Q_1 Q_2 k}{(Q_1 Q_2 k^2 + 1)n} \\ -\frac{j Q_1 Q_2 k}{(Q_1 Q_2 k^2 + 1)n} & \frac{Q_2}{(Q_1 Q_2 k^2 + 1)n^2} - \frac{j}{n^2} \end{pmatrix} \tag{4}$$

where $Q_1$ and $Q_2$ are the quality factors of the source and receiver coils, respectively; $k$ is the coupling coefficient, where $k = M_{sr}/\sqrt{L_S L_r}$; the other variables are based on [35]; and $n$ is the transformer ratio, where $n = \sqrt{L_S/L_r}$. Thus, the expression of the conjugate image impedances is

$$Z_{PP\_C_S} = \left( \frac{Q_1}{\sqrt{Q_1 Q_2 k^2 + 1}} + j \right) X_o, \tag{5}$$

$$Z_{PP\_C_r} = \left( \frac{Q_2}{n^2 \sqrt{Q_1 Q_2 k^2 + 1}} + \frac{j}{n^2} \right) X_o. \tag{6}$$

$Z_{PP\_C_S}$ and $Z_{PP\_C_r}$ clearly have a non-zero imaginary part. Thus, a compensating reactance should be added on both ports. In particular, the parameters that recognize the optimum design are as follows:

$$X_{PP\_C_S} = \omega L_S, \tag{7}$$

$$X_{PP\_C_r} = \omega L_r, \tag{8}$$

$$L_{cs,PP} = \frac{\sqrt{Q_1 Q_2 k^2 + 1}\, R_o}{\omega_o\, Q_1}, \tag{9}$$

$$L_{cr,PP} = \frac{\sqrt{Q_1 Q_2 k^2 + 1}\, R_L}{\omega_o\, Q_2}, \tag{10}$$

where $R_o$ is the input impedance.

## 5. STLC and MTCWC Experiment Topology

The proposed system is intended for charging low-power-consumption home appliances, such as smartphones, shavers, and toothbrushes. However, the proposed STLC-based topology generates stronger leakage magnetic fields than MTCWC because it does not have any shielding to reduce the leakage magnetic fields [10]. The implemented circuit design of the proposed STLC is shown in Figure 6. The STLC is set with 6 and 15 cm air gaps to measure transfer distance, power, and efficiency when the system is loaded. The transfer power and efficiency are recorded, relative to the transfer distance, as seen in the results section. Measurements are taken at the source and receiving coils with a digital multi-meter (DT9205, Dowdon, Shenzhen, China), an oscilloscope (MCP lab electronics/DQ7042C, Shanghai MCP Corp., Shanghai, China), a digital multi-meter (MCP lab electronics/MT8045, Shanghai MCP Corp., Shanghai, China), and a traditional distance meter (0–40 cm). Load resistances of 20, 50, and 100 Ω are used to test the power delivery capabilities at the receiver circuit. A DC power supply (GPS-3030D, Cole-Parmer, Stone, UK) is used to supply the source circuit. The specifications of the source and receiver coils of the proposed STLC system are shown Table 2. The same circuit can be used here for the STLC without a load. The proposed STLC system introduces another advantage by using MTCWC, which is located in the center of the single turn coil of the receiver (Figure 7a), and the proposed coil of MTCWC (Figure 7b). The MTCWC can be used for charging mobile phones (Figure 8). The parameters that can be used for the receiver coils are shown in Table 3, while the parameters for the source coil are shown in Table 2.
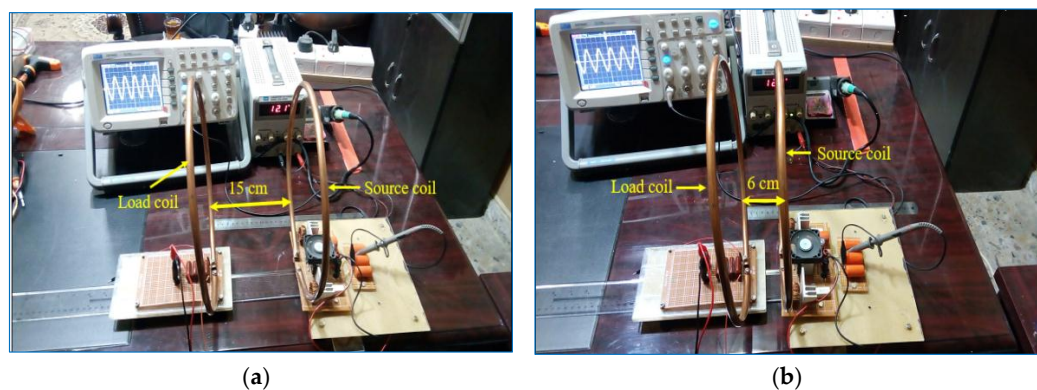


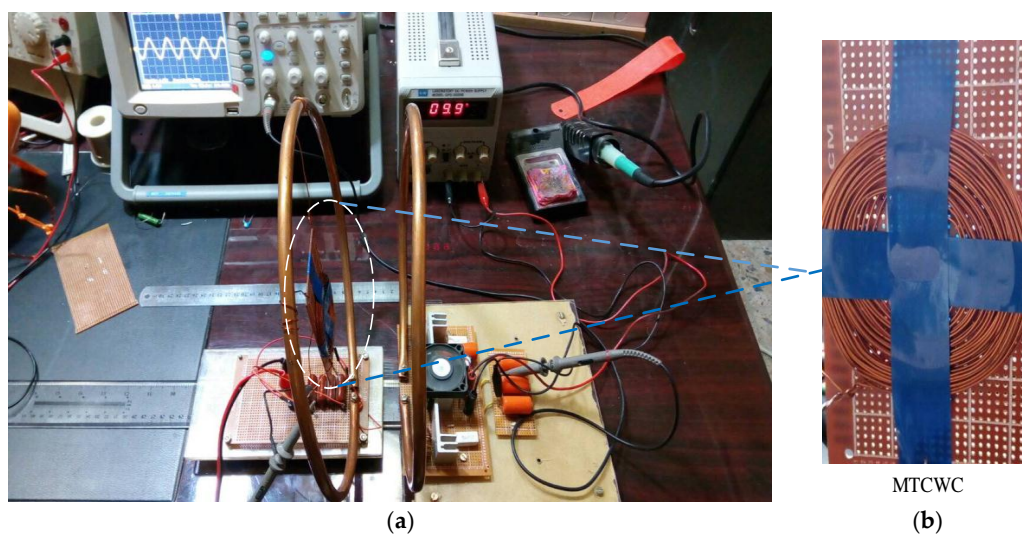**Figure 6.** Experiment topology of STLC with a load at (**a**) 6 cm and (**b**) 15 cm.



**Figure 7.** Experiment topology of MTCWC of (**a**) the adopted experiment and (**b**) MTCWC circuit.
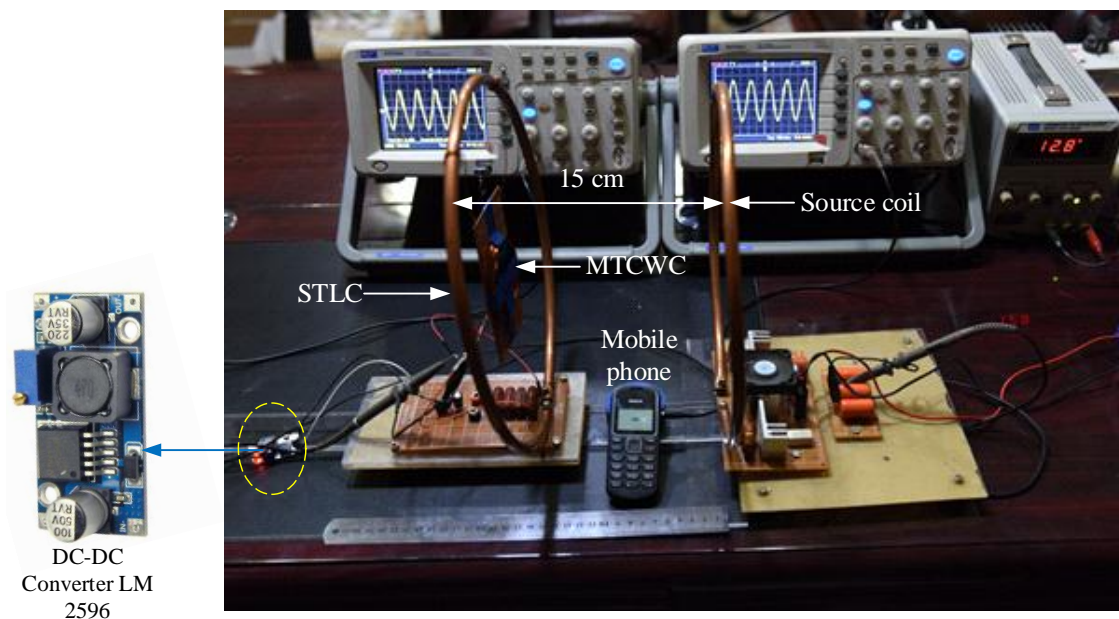
**Figure 8.** MTCWC during mobile charging.

**Table 2.** Specification of transmitter and receiver coils.

| Specification | Source and Receiver Coils |
|---|---|
| Number of turns | Single loop |
| Diameter of turn (cm) | 30 |
| Thickness of coil (cm) | 0.1 |
| Diameter of metal conductor | 0.958 |
| Air gap between coils (cm) | 1–30 |

**Table 3.** Parameters of MTCWC.

| Specification | MTCWC |
|---|---|
| Number of turns | 45 |
| Diameter of coil (cm) | 5.7 |
| Diameter of wire | 0.8 |
| Inductance (μH) | 95 |
| Air gap between (cm) | 1–30 |

## 6. Experimental Results and Discussion

### 6.1. STLC Results

When the experimental setting was completed, the DC power of the source coil was turned on. The voltage signal, with its frequency spectrum measured from the oscilloscope at the transmitter coil, is shown in Figure 9a. The prototype of the STLC source circuit was built to resonate at 1 MHz, and the frequency spectrum was set in pure tone (i.e., sinusoidal). The signals detected by the resonant circuit at the receiver, in which the frequency spectra were measured at 6 cm and 15 cm, with resistance loads of 100 Ω, are shown in Figure 9b,c. A clear sine wave and a pure tone were observed in the frequency spectra at both distances. The main results of the proposed STLC method are shown in Figures 10 and 11. To establish the relationship, the transfer distances in centimeters are plotted on the *x*-axis, and the output powers (in watts), or transfer efficiencies (in percentage), are plotted on the *y*-axis. The output power decreased when the transfer distance increased (Figure 10). For the proposed STLC, an output power of 4.84 W was obtained at the transfer distance of 2 cm with a load

of 100 Ω. The output power sufficiently charged the smartphones (i.e., iPhone 7 and iPhone 7 Plus), toothbrushes, and shavers. Therefore, the STLC system can be used to charge low-power devices. Meanwhile, laptops need more than 120 W of power. Spikes in the output power and transfer efficiency are shown in Figures 10 and 11, respectively. The spikes appear at the 20 Ω resistive load at 4–9 cm. To accomplish peak transfer power and efficiency, impedance matching between transmitter and receiver coils is crucial. When the distance was changed between the transmitter and receiver coils, the coupling factor was adjusted accordingly, which resulted in a change in the ideal impedance ratio. Thus, transfer power and efficiency experienced an increase–maximum–decrease trend in the range of 4–9 cm in the current work. Then, both parameters deteriorated when the distance increased. The other conclusions of the current work are consistent with the findings in the literature [36–42].

The correlation between transfer efficiency and transfer distance is shown in Figure 11. The relationship between transfer distance and output power is established by two experiments, namely, with and without loads. The efficiency percentage is based on the ratio of the measured output power to the measured input power. The transfer efficiencies vary from 8.4% to 80.66% for the experiment with a 100 Ω resistive load and from 11.45% to 88.54% for the experiment without a load when the distances shift from 1 cm to 30 cm. The transfer efficiency of the STLC system without a load was 9% better than that with the load. However, the transfer efficiency of the loaded device was limited to 66.66% at 6 cm for the STLC system.

The relationships between three parameters are shown in Figure 12a–c: (i) Measured output power; (ii) transfer efficiency; and (iii) distance for the three loads of 20, 50, and 100 Ω. The transfer power and efficiency in Figure 12c (resistive load of 100 Ω) are better than those in Figure 12a,b (resistive loads of 20 Ω and 50 Ω, respectively) due to the high resistive load that resulted in a low voltage drop across the load resistance (i.e., 100 Ω). The worst case, which can be explained by the low resistive load (20 Ω), is represented in Figure 12a. Thus, when distance increases, transfer efficiency and power decrease, and vice versa. The maximum transfer powers and efficiencies were observed at the short distances of 1–6 cm for 100 Ω, 1–8 cm for 50 Ω, and 6–8 cm for 20 Ω, as shown by the red and dark red markers in Figure 12. The orange, yellow, and green markers in the figure indicate the mid-range values of transfer power and efficiency, while the light blue and blue markers denote the low transfer power and efficiency caused by the increase in transfer distance, especially at 20 Ω of resistive load.
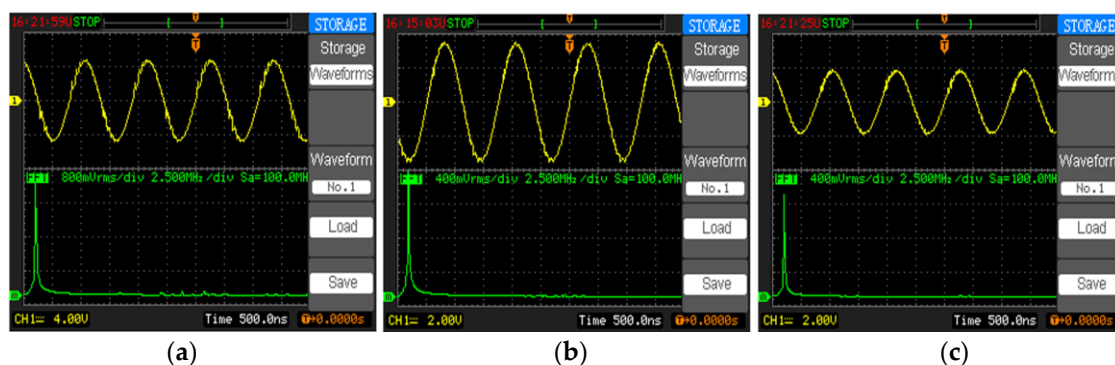


**Figure 9.** Waveform and frequency spectra of (**a**) a source circuit measured at the source coil; (**b**) measured signals at the receiver coil for the system with a resistive load of 100 Ω at 6 cm; and (**c**) measured signals at the receiver coil for the system with a resistive load of 100 Ω at 15 cm.
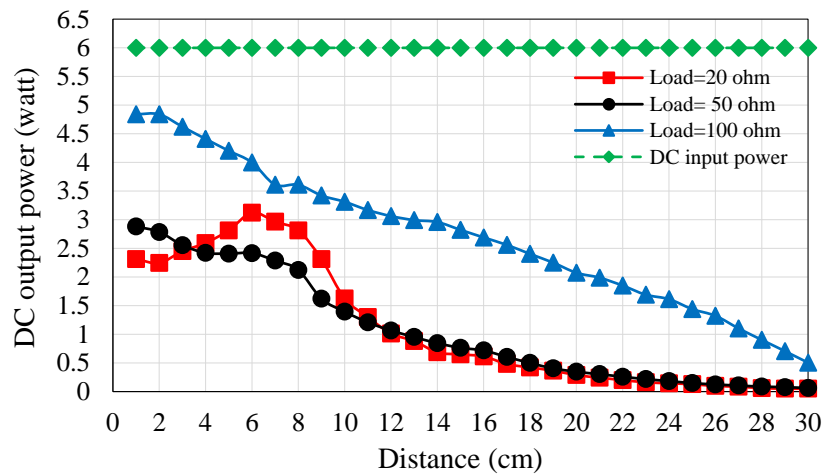
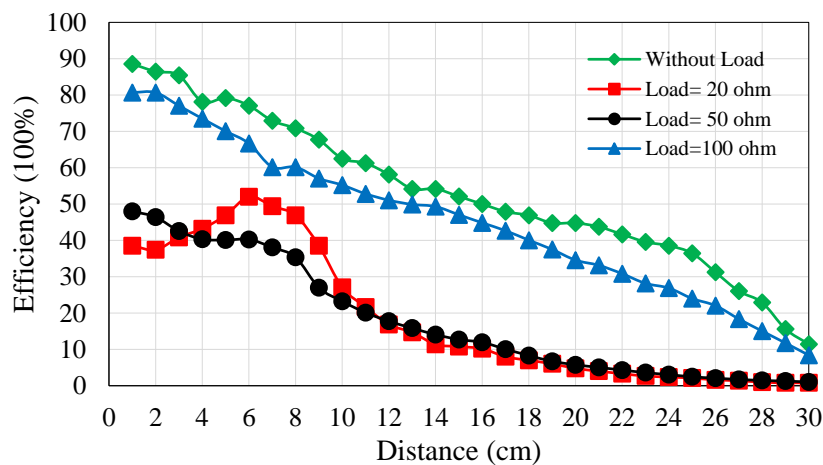**Figure 10.** The relationship between output power and transfer distance.



**Figure 11.** The relationship between transfer efficiency and transfer distance, with and without a load.
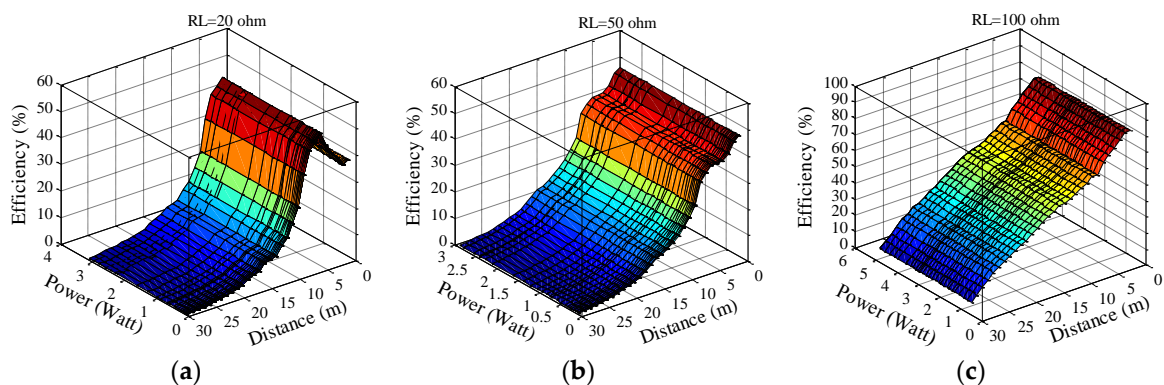


**Figure 12.** The relationship between output power and transfer efficiency versus distance with the following loads: (**a**) 20 Ω; (**b**) 50 Ω; and (**c**) 100 Ω.

*6.2. MTCWC Results*

Similar to those of the STLC experiment, the results of the proposed MTCWC experiment were investigated. The same source and transmitter circuits were used for STLC and MTCWC. The source voltage signal and its frequency spectrum were previously generated (see Figure 9a). The voltage signals and frequency spectra of the MTCWC receiver circuits, with air gaps of 6 cm and 15 cm

between the sources and receiver coils, are shown in Figure 13a,b, respectively. The tested MTCWC, when the resistance load was 100 Ω at the receiver circuit, is shown in Figure 13b,c. To further investigate the MTCWC performance metrics, the receiver circuits were tested with different loads: 20, 50, and 100 Ω. A pure tone of the frequency spectrum was observed at distances of 6 and 15 cm. However, the voltage signal of the MTCWC was slightly distorted, relative to that of the STLC. The main results of the prototype testing of the proposed MTCWC are shown in Figures 14 and 15. As shown in Figure 14, the output power decreases when the transfer distance increases. In the proposed MTCWC configuration, an output power of 2.6 W can be measured at the transfer distance of 1 cm when the load is 100 Ω. The output power (i.e., 2.6 W) sufficiently charged a low-power mobile phone (i.e., Nokia 1280, as shown in Figure 8), a shaver, and a toothbrush. Therefore, the MTCWC system can be used to charge low-power devices. The relationship between transfer efficiency and transfer distance is shown in Figure 15. This Figure clarifies the correlation between transfer efficiency and transfer distance, derived from the two experiments (i.e., with and without loads). The efficiency percentage corresponds to the ratio of measured output power to measured input power. As shown in Figure 15, the transfer efficiencies vary from 1.68% to 43.2% with a load of 100 Ω, and from 18.22% to 90.62% without a load when the distance is adjusted from 1 cm to 30 cm, respectively. The transfer efficiency of the MTCWC system without a load is better than that with the load. However, the transfer efficiency was limited to 33.6% at 6 cm and 100 Ω for the MTCWC system. The output power and transfer efficiency of the STLC are two times better than those of the MTCWC.
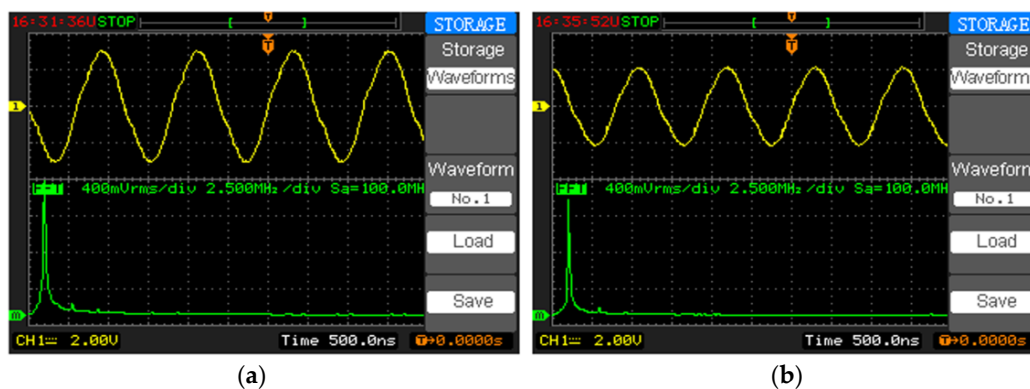


(**a**)  (**b**)

**Figure 13.** Measured voltage signals and frequency spectra at the receiver coil when the system is loaded with resistive loads of 100 Ω at (**a**) 6 cm and (**b**) 15 cm.
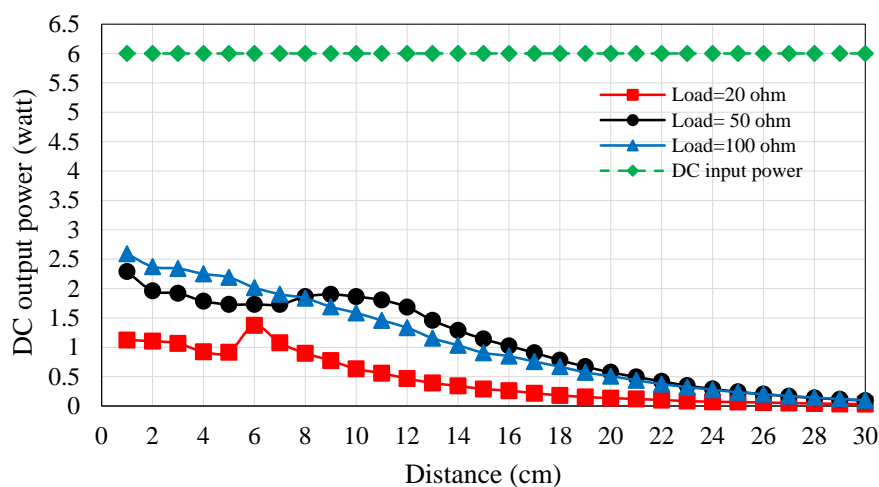


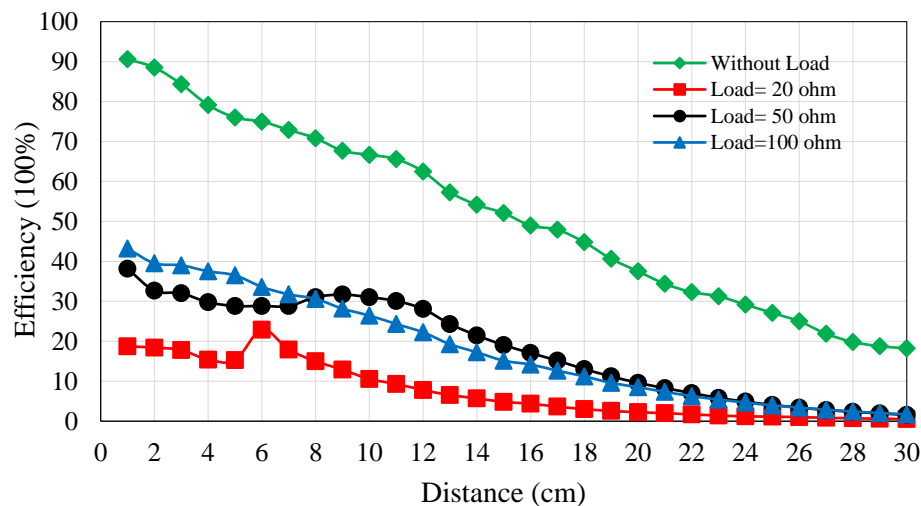**Figure 14.** The relationship between output power and transfer distance.

**Figure 15.** The relationship between transfer efficiency and transfer distance, with and without load.

Similar to the STLC, the relationship in three dimensions was established for the MTCWC to investigate the correlation between transfer distance, on the one hand, and transfer efficiency and output power, on the other hand. The results of the correlation are presented in Figure 16a–c for the system with loads of 20, 50, and 100 Ω, respectively. The transfer power and efficiency in Figure 16c (resistive load of 100 Ω) are better than those in Figure 16b,c (resistive loads of 20 and 50 Ω). The worst case, which can be attributed to the low resistive load of 20 Ω, is shown in Figure 16a. Thus, when the distance increases, the transfer efficiency and output power decrease, and vice versa. The maximum transfer power and efficiency values can be observed at short distances of 1–5 cm for 100 Ω, 1 cm and 8–12 cm for 50 Ω, and 6 cm for 20 Ω, as shown by the red and dark red markers in Figure 16. The orange, yellow, and green markers represent the mid-range values of transfer power and efficiency. The light blue and blue markers denote the low transfer power and efficiency caused by the increase in transfer distance, especially at 20 Ω resistive load.

The overall results indicate that STLC has better performance metrics (transfer power and efficiency) than MTCWC. The STLC design comprises a larger receiver coil, as compared to the MTCWC design. In addition, STLC is precisely aligned with the transmitter coil, unlike the MTCWC. MTCWC was used to charge a mobile phone (Figure 8), and the charging process was achieved at the distance range of 1–15 cm (i.e., air gap) between transmitter and receiver coils. The AC and DC output voltages are shown in Figure 17a,b, respectively. The DC output voltages were recorded during the charging process, and they were 5 V, based on the oscilloscope measurement (Figure 17b). The voltage value was sufficient for charging the mobile phone. However, both MTCWC and STLC methods have certain limitations, in terms of improving the abovementioned parameters. First, transfer power always varies when charging mobile devices due to misalignment; thus, transfer efficiency is not always constant and may decrease. Therefore, the collected energy is suitable only for supplying low-power devices or sensors and cannot be used for high-power applications. Second, transfer energy can be increased by increasing the power of the source coil. However, in medical applications, power and operating frequency cannot be increased when transferring the maximum power to a load device because of the increased power and frequency on human tissues. The permissible exposure level should be followed to avoid exposing the human body to electromagnetic waves.
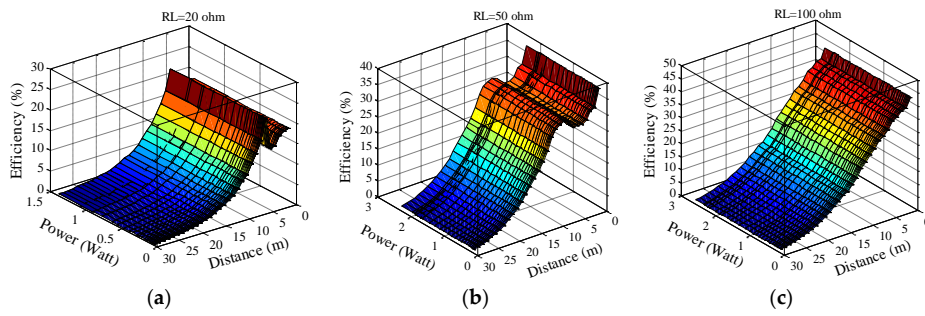
**Figure 16.** The relationship between output power and transfer efficiency versus distance with the following loads: (**a**) 20 Ω; (**b**) 50 Ω; and (**c**) 100 Ω.
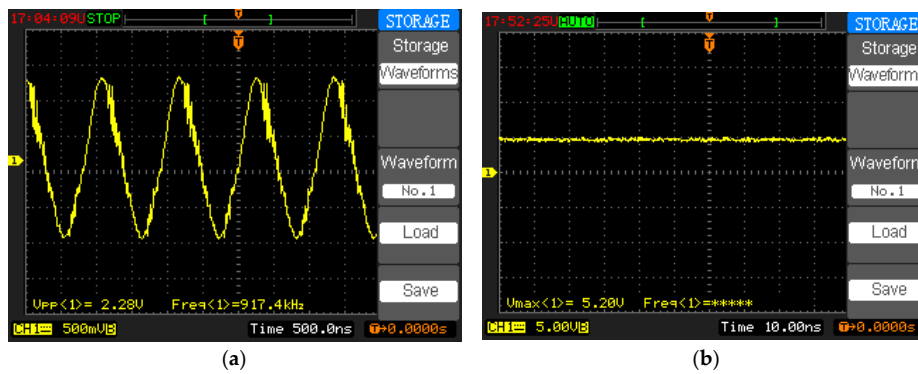


**Figure 17.** Oscilloscope measurement of (**a**) AC voltage and (**b**) DC voltage.

## 7. Comparison with the Literature

Several studies on WPTs have been published, and some can be compared with our proposed systems (Table 4). The previous systems used copper wire coils in their prototypes. The proposed methods outperform the prototypes of some previous studies [5,13,16,43–46], in terms of transfer distance, output power, and transfer efficiency. The findings of other past studies [47,48] are consistent with the results of our current work.

**Table 4.** Comparison between the two proposed systems (STLC and MTCWC) and previous systems.

| Ref. | Frequency (kHz) | Transfer Distance (cm) | $P_{in}$ (W) | $P_{out}$ (W) (with Load) | $\eta$ (%) (with Load) | Type of Coils |
|---|---|---|---|---|---|---|
| [43]/2012 | 1.300 | 4.4 | 1.05 | 0.475 | 45.01 | Copper wire coil |
| [13]/2013 | 29–32 | 1.5 | 1.25 | 0.5 | 40 | Copper wire coil |
| [49]/2013 | 500 | 13 | 0.03 | 1.2 | 40 | Copper wire coil |
| [44]/2014 | 3800 | 5 | 0.14 | 0.042 | 30 | Single tube loop coil |
| [5]/2014 | 1000 | 10 | 0.056 | 3 | 53 | Copper wire coil |
| [48]/2014 | 0.1–0.2 | 0.5 | 7.14 | 5–120 | 70 | Copper wire coil |
| [47]/2015 | 97.56 | N/A | 6.92 | 4.5 | 65 | Copper wire coil |
| [16]/2015 | 6.78 | 1.04 | 0.3 | 0.1 | 30 | Copper wire coil |
| [45]/2016 | 0.097 | 0.06 | 6 | 3.1 | 48.2–51.2 | Copper wire coil |
| [46]/2017 | 13.56 | 2.25 | 6.7 | 2.8 | 41.7 | Copper wire coil |
| STLC (this work) | 1000 | 2, 6 and 15 | 6 | 4.84 @ 2 cm<br>4 @ 6 cm<br>2.82 @ 15 cm | 80.66 @ 2 cm<br>66.66 @ 6 cm<br>47.04 @ 15 cm | Single tube loop coil |
| MTCWC (this work) | 1000 | 2, 6 and 15 | 6 | 2.37 @ 2 cm<br>2 @ 6 cm<br>0.908 @ 15 cm | 39.52 @ 2 cm<br>33.6 @ 6 cm<br>15.13 @ 15 cm | Multi turn copper wire coil |

## 8. Conclusions

In this study, STLC and MTCWC systems are proposed to deliver power to low-power-consumption devices. Both designs are implemented using an STLC coil in the transmitting and receiving circuits and an MTCWC in the receiver circuit. Three loads are used to test the performance metrics of the system, namely, 20 Ω, 50 Ω, and 100 Ω. The transfer power and efficiency are investigated at 2, 6, and 15 cm for all loads. The transfer power and efficiency are optimal at a 100 Ω resistive load. The corresponding transfer powers and efficiencies for STLC are 4.84 W and 80.66% at 2 cm, 4 W and 66.66% at 6 cm, and 2.82 W and 47.04% at 15 cm. Meanwhile, the corresponding transfer powers and efficiencies for MTCWC are 2.37 W and 39.52% at 2 cm, 2 W and 33.6% at 6 cm, and 0.908 W and 15.13% at 15 cm. Our experimental study proves that the STLC design is better than the MTCWC design, in terms of transfer power and efficiency. The MTCWC prototype can be used to charge mobile phones at 1–15 cm air gaps between transmitter and receiver coils. The results further reveal that charging power and efficiency decrease with distance. In addition, the proposed STLC and MTCWC outperform previous systems that use copper wire and tube loop coils, in terms of transfer power, efficiency, and distance, especially without a load. In the proposed designs, more than one device can be charged simultaneously. Future work may consider the adoption of MTCWC for a transmitter circuit to efficiently charge the battery of certain applications, such as drones and headphones, thereby increasing the lifetime of the battery.

## References

1. Campi, T.; Cruciani, S.; Feliziani, M. Wireless power transfer technology applied to an autonomous electric uav with a small secondary coil. *Energies* **2018**, *11*, 352. [CrossRef]
2. Mmc Technologies. Available online: http://www.Mmcuav.Com/about/company/ (accessed on 27 August 2017).
3. Shinohara, N.; Shinohara, N. History, present and future of wpt. In *Wireless Power Transfer via Radiowaves*; John Wiley & Sons, Inc.: Hoboken, NJ, USA, 2013; pp. 1–20.
4. Mittleider, A.; Griffin, B.; Detweiler, C. *Experimental Analysis of a Uav-Based Wireless Power Transfer Localization System*; Experimental Robotics; Springer: Berlin, Germany, 2016; pp. 357–371.
5. Jadidian, J.; Katabi, D. Magnetic MIMO: How to charge your phone in your pocket. In Proceedings of the 20th Annual International Conference on Mobile Computing and Networking 2014, Maui, HI, USA, 7–11 September 2014; pp. 495–506.
6. Kawashima, N.; Takeda, K. Laser energy transmission for a wireless energy supply to robots. In *Robotics and Automation in Construction*; InTech: London, UK, 2008.
7. Kawashima, N.; Takeda, K.; Yabe, K. Possible utilization of the laser energy transmission in space. *Trans. Jpn. Soc. Aeron. Space Sci. Aerosp. Technol. Jpn.* **2012**, *10*, Tq_1–Tq_3. [CrossRef]
8. Mai, R.; Ma, L.; Liu, Y.; Yue, P.; Cao, G.; He, Z. A maximum efficiency point tracking control scheme based on different cross coupling of dual-receiver inductive power transfer system. *Energies* **2017**, *10*, 217. [CrossRef]
9. Pinuela, M.; Yates, D.C.; Lucyszyn, S.; Mitcheson, P.D. Maximizing dc-to-load efficiency for inductive power transfer. *IEEE Trans. Power Electron.* **2013**, *28*, 2437–2447. [CrossRef]
10. Park, J.; Kim, D.; Hwang, K.; Park, H.H.; Kwak, S.I.; Kwon, J.H.; Ahn, S. A resonant reactive shielding for planar wireless power transfer system in smartphone application. *IEEE Trans. Electromagn. Compat.* **2017**, *59*, 695–703. [CrossRef]

11. Feng, J.; Li, Q.; Lee, F.C. Omnidirecitional wireless power transfer for portable devices. In Proceedings of the International Conference of Applied Power Electronics Conference and Exposition (APEC), Tampa, FL, USA, 26–30 March 2017; pp. 1675–1681.

12. Goguri, S.; Mudumbai, R.; Kruger, A. Optimizing Wireless Power Transfer with Multiple Transmitters. In Proceedings of the IEEE International Conference on Information Sciences and Systems (CISS), Baltimore, MD, USA, 22–24 March 2017; pp. 1–5.

13. Li, Y.; Li, X.; Peng, F.; Zhang, H.; Guo, W.; Zhu, W.; Yang, T. Wireless energy transfer system based on high q flexible planar-litz mems coils. In Proceedings of the 2013 8th IEEE International Conference on, Nano/Micro Engineered and Molecular Systems (NEMS), Suzhou, China, 7–10 April 2013; pp. 837–840.

14. Jonah, O.; Georgakopoulos, S.V.; Tentzeris, M.M. Orientation insensitive power transfer by magnetic resonance for mobile devices. In Proceedings of the International Conference of Wireless Power Transfer (WPT), Perugia, Italy, 15–16 May 2013; pp. 5–8.

15. Ye, Z.-H.; Sun, Y.; Dai, X.; Tang, C.-S.; Wang, Z.-H.; Su, Y.-G. Energy efficiency analysis of u-coil wireless power transfer system. *IEEE Trans. Power Electron.* **2016**, *31*, 4809–4817. [CrossRef]

16. Kim, J.; Kim, D.-H.; Choi, J.; Kim, K.-H.; Park, Y.-J. Free-positioning wireless charging system for small electronic devices using a bowl-shaped transmitting coil. *IEEE Trans. Microw. Theory Tech.* **2015**, *63*, 791–800. [CrossRef]

17. Fu, M.; Zhang, T.; Zhu, X.; Luk, P.C.-K.; Ma, C. Compensation of cross coupling in multiple-receiver wireless power transfer systems. *IEEE Trans. Ind. Inform.* **2016**, *12*, 474–482. [CrossRef]

18. De Rooij, M.A.; Mirenda, A. Automotive compatible single amplifier multi-mode wireless power for mobile devices. In Proceedings of the 2nd Vehicular Technology Conference (VTC Fall), Boston, MA, USA, 6–9 September 2015; pp. 1–5.

19. Rozman, M.; Fernando, M.; Adebisi, B.; Rabie, K.M.; Collins, T.; Kharel, R.; Ikpehai, A. A new technique for reducing size of a wpt system using two-loop strongly-resonant inductors. *Energies* **2017**, *10*, 1614. [CrossRef]

20. Desai, N.; Chandrakasan, A.P. A zvs resonant receiver with maximum efficiency tracking for device-to-device wireless charging. In Proceedings of the 42nd European Solid-State Circuits Conference (ESSCIRC Conference 2016, Lausanne, Switzerland, 12–15 September 2016; pp. 313–316.

21. Mao, F.; Lu, Y.; Seng-Pan, U.; Martins, R.P. A reconfigurable cross-connected wireless-power transceiver for bidirectional device-to-device charging with 78.1% total efficiency. In Proceedings of the IEEE International Solid-State Circuits Conference-(ISSCC), San Francisco, CA, USA, 11–15 February 2018; pp. 140–142.

22. Integrated Device Technology (Idt). Available online: https://www.Idt.Com/products/power-management/wireless-power/introduction-to-wireless-battery-charging (accessed on 29 October 2017).

23. Jawad, A.M.; Nordin, R.; Gharghan, S.K.; Jawad, H.M.; Ismail, M. Opportunities and challenges for near-field wireless power transfer: A review. *Energies* **2017**, *10*, 1022. [CrossRef]

24. Jiang, H.; Zhang, J.; Lan, D.; Chao, K.K.; Liou, S.; Shahnasser, H.; Fechter, R.; Hirose, S.; Harrison, M.; Roy, S. A low-frequency versatile wireless power transfer technology for biomedical implants. *IEEE Trans. Biomed. Circ. Syst.* **2013**, *7*, 526–535. [CrossRef] [PubMed]

25. Elnail, K.; Huang, X.; Xiao, C.; Tan, L.; Haozhe, X. Core structure and electromagnetic field evaluation in wpt systems for charging electric vehicles. *Energies* **2018**, *11*, 1734. [CrossRef]

26. Pantic, Z.; Lukic, S.M. Framework and topology for active tuning of parallel compensated receivers in power transfer systems. *IEEE Trans. Power Electron.* **2012**, *27*, 4503–4513. [CrossRef]

27. Zhang, W.; Wong, S.-C.; Chi, K.T.; Chen, Q. Analysis and comparison of secondary series-and parallel-compensated inductive power transfer systems operating for optimal efficiency and load-independent voltage-transfer ratio. *IEEE Trans. Power Electron.* **2014**, *29*, 2979–2990. [CrossRef]

28. Lee, S.-H.; Lorenz, R.D. Development and validation of model for 95%-efficiency 220-w wireless power transfer over a 30-cm air gap. *IEEE Trans. Ind. Appl.* **2011**, *47*, 2495–2504. [CrossRef]

29. Dionigi, M.; Costanzo, A.; Mongiardo, M. Network Methods for Analysis and Design of Resonant Wireless Power Transfer Systems. 2012. Available online: https://www.intechopen.com/books/wireless-power-transfer-principles-and-engineering-explorations/networks-methods-for-the-analysis-and-design-of-wireless-power-transfer-systems (accessed on 10 October 2017). [CrossRef]

30. Oh, K.-S.; Lee, W.-S.; Lee, W.-S.; Yu, J.-W. A capacitor-loaded cylindrical resonant coil with parallel connection. *Appl. Phys. Lett.* **2012**, *101*, 064105. [CrossRef]

31. Junaid, A.B.; Lee, Y.; Kim, Y. Design and implementation of autonomous wireless charging station for rotary-wing uavs. *Aerosp. Sci. Technol.* **2016**, *54*, 253–266. [CrossRef]

32. Junaid, A.B.; Konoiko, A.; Zweiri, Y.; Sahinkaya, M.N.; Seneviratne, L. Autonomous wireless self-charging for multi-rotor unmanned aerial vehicles. *Energies* **2017**, *10*, 803. [CrossRef]

33. Liu, X.; Wang, T.; Yang, X.; Jin, N.; Tang, H. Analysis and design of a wireless power transfer system with dual active bridges. *Energies* **2017**, *10*, 1588. [CrossRef]

34. Monti, G.; Costanzo, A.; Mastri, F.; Mongiardo, M. Optimal design of a wireless power transfer link using parallel and series resonators. *Wirel. Power Transf.* **2016**, *3*, 105–116. [CrossRef]

35. Inagaki, N. Theory of image impedance matching for inductively coupled power transfer systems. *IEEE Trans. Microw. Theory Tech.* **2014**, *62*, 901–908. [CrossRef]

36. Jonah, O.; Georgakopoulos, S.V. Wireless power transfer in concrete via strongly coupled magnetic resonance. *IEEE Trans. Antennas Propag.* **2013**, *61*, 1378–1384. [CrossRef]

37. Qingxin, Y.; Xian, Z.; Haiyan, C.; Yang, L.; Liang, J.; Rongge, Y. Direct field-circuit coupled analysis and corresponding experiments of electromagnetic resonant coupling system. *IEEE Trans. Magn.* **2012**, *48*, 3961–3964. [CrossRef]

38. Calder, R.J.; Lee, S.-H.; Lorenz, R.D. Efficient, mhz frequency, resonant converter for sub-meter (30 cm) distance wireless power transfer. In Proceedings of the IEEE International Conference on Energy Conversion Congress and Exposition (ECCE), Denver, CO, USA, 15–19 September 2013; pp. 1917–1924.

39. Park, J.; Tak, Y.; Kim, Y.; Kim, Y.; Nam, S. Investigation of adaptive matching methods for near-field wireless power transfer. *IEEE Trans. Antennas Propag.* **2011**, *59*, 1769–1773. [CrossRef]

40. Vijayakumaran Nair, V.; Choi, J.R. An efficiency enhancement technique for a wireless power transmission system based on a multiple coil switching technique. *Energies* **2016**, *9*, 156. [CrossRef]

41. Abatti, P.J.; Pichorim, S.F.; de Miranda, C.M. Maximum power transfer versus efficiency in mid-range wireless power transfer systems. *J. Microw. Optoelectron. Electromagn. Appl.* **2015**, *14*, 97–109. [CrossRef]

42. Fu, M.; Yin, H.; Zhu, X.; Ma, C. Analysis and tracking of optimal load in wireless power transfer systems. *IEEE Trans. Power Electron.* **2015**, *30*, 3952–3963. [CrossRef]

43. Seo, Y.-S.; Hughes, Z.; Hoang, M.; Isom, D.; Nguyen, M.; Rao, S.; Chiao, J.-C. Investigation of wireless power transfer in through-wall applications. In Proceedings of the IEEE Microwave Conference Proceedings (APMC), 2012 Asia-Pacific, Kaohsiung, Taiwan, 4–7 December 2012; pp. 403–405.

44. Kallel, B.; Keutel, T.; Kanoun, O. Miso configuration efficiency in inductive power transmission for supplying wireless sensors. In Proceedings of the 2014 11th International Multi-Conference on IEEE Systems, Signals & Devices (SSD), Barcelona, Spain, 11–14 February 2014; pp. 1–5.

45. Worgan, P.; Knibbe, J.; Fraser, M.; Martinez Plasencia, D. Powershake: Power transfer interactions for mobile devices. In Proceedings of the ACM 2016 CHI Conference on Human Factors in Computing Systems, San Jose, CA, USA, 7–12 May 2016; pp. 4734–4745.

46. Chen, J.-F.; Ding, Z.; Hu, Z.; Wang, S.; Cheng, Y.; Liu, M.; Wei, B.; Wang, S. Metamaterial-based high-efficiency wireless power transfer system at 13.56 mhz for low power applications. *Prog. Electromagn. Res.* **2017**, *72*, 17–30. [CrossRef]

47. Zhong, W.; Hui, S. Maximum energy efficiency tracking for wireless power transfer systems. *IEEE Trans. Power Electron.* **2015**, *30*, 4025–4034. [CrossRef]

48. Bululukova, D.; Kramer, M. Application of existing wireless power transfer standards in automotive applications. In Proceedings of the IEEE International Conference on Connected Vehicles and Expo (ICCVE), Vienna, Austria, 3–7 November 2014; pp. 863–864.

49. Lee, E.; Huh, J.; Thai, X.; Choi, S.; Rim, C. Impedance transformers for compact and robust coupled magnetic resonance systems. In Proceedings of the IEEE Energy Conversion Congress and Exposition (ECCE), Denver, CO, USA, 15–19 September 2013; pp. 2239–2244.